13:02:25 OCA PAD INITIATION - PROJECT HEADER INFORMATION 12/20/96

Active

Project #: G-35-W15 Cost share #: G-35-382 Rev #: 0
Center # : 10/24-6-R0213-0A0 Center shr #: 10/22-1-F0213-0A0 OCA file #:
Work type : RES
Contract#: 49Y-FHW69V Mod #: INITIATION Document : CONT
Prime #: DE-AC05-840R21400 Contract entity: GTRC

Subprojects ? : N CFDA:
Main project #: PE #:

Project unit: E & A SCI Unit code: 02.010.140
Project director(s):
LONG L T E & A SCI (404)894-2860

Sponsor/division names: OAK RIDGE NAT'L LAB / LOCKHEED-MARTIN
Sponsor/division codes: 240 / 001

Award period: 961202 to 971201 (performance) 971201 (reports)

Sponsor amount	New this change	Total to date
Contract value	20,018.00	20,018.00
Funded	20,018.00	20,018.00
Cost sharing amount		2,500.00

Does subcontracting plan apply ?: N

Title: NUMERICAL CALCULATIONS FOR SCATTERING OF SEISMIC WAVES FROM SPHERES

PROJECT ADMINISTRATION DATA

OCA contact: Anita D. Rowland 894-4820

Sponsor technical contact

DR. WILLIAM DOLL
(423)576-9930

OAK RIDGE NATIONAL LABORATORY
LOCKHEED MARTIN ENERGY SYSTEMS, INC.
P.O. BOX 2002
OAK RIDGE, TN 37831

Sponsor issuing office

JANICE J. CRIPPEN
(423)576-4415

OAK RIDGE NATIONAL LABORATORY
LOCKHEED MARTIN ENERGY SYSTEMS, INC.
PROCUREMENT DIVISION
P.O. BOX 2002
OAK RIDGE, TN 37831-6501

Security class (U,C,S,TS) : U ONR resident rep. is ACO (Y/N): N
Defense priority rating : supplemental sheet
Equipment title vests with: Sponsor X GIT
NONE ANTICIPATED
Administrative comments -
INITIATION OF 1-YR AGREEMENT.

4
2

SR043

Closeout Notice Date 05-DEC-1997

Project Number G-35-W15 Doch Id 39871

Center Number 10/24-6-R0213-0A0

Project Director LONG, LELAND

Project Unit E & A SCI

Sponsor OAK RIDGE NAT'L LAB/MARTIN MARIETTA

Division Id 4868

Contract Number 49Y-FHW69V Contract Entity GTRC

Prime Contract Number DE-AC05-840R21400

Title NUMERICAL CALCULATIONS FOR SCATTERING OF SEISMIC WAVES FROM SPHERES

Effective Completion Date 01-DEC-1997 (Performance) 01-DEC-1997 (Reports)

Closeout Action:	Y/N	Date Submitted
Final Invoice or Copy of Final Invoice	Y	
Final Report of Inventions and/or Subcontracts	Y	
Government Property Inventory and Related Certificate	Y	
Classified Material Certificate	N	
Release and Assignment	N	
Other	N	

Comments

Distribution Required:

Project Director/Principal Investigator	Y
Research Administrative Network	Y
Accounting	Y
Research Security Department	N
Reports Coordinator	Y
Research Property Team	Y
Supply Services Department/Procurement	Y
Georgia Tech Research Corporation	Y
Project File	Y

NOTE: Final Patent Questionnaire sent to PDPI

G-35-W15
#1

Final Report

Project G-35-w15

Numerical Calculation for Scattering of Seismic Waves from Spheres

(a study: Scattered Waves Generated by a Small Subsurface Scatterer)

by Xiuqi Chen and L.T. Long

School of Earth and Atmospheric Sciences

Georgia Institute of Technology

Atlanta, GA 30318-0340

Prepared for

Oak Ridge National Laboratory

Lockhead-Martin Energy Systems Incs

P.O. Box 2002

Oak Ridge, TN 37831

1 December 1997

Scattered Waves Generated by a Small Subsurface Scatterer

1. Introduction

Seismic scattering by a spherical inhomogeneity has been studied by several workers. Using the equivalent source method and and the Born approximation, Wu and Aki (1985) developed a series of formula to calculate the scattered wave field generated by a spherical inhomogeneity having a small impedance contrast with the surrounding medium. The exact solution for any impedance contrast is given by Mie theory, in which the solution is obtained in the form of an infinite series (Ying and Truell, 1956). Using Mie theory, Tie (1987) investigated the scattered wavefield of a plane longitudinal wave incident on a spherical obstacle. Several different types of obstacles were studied in Tie's work, including a rigid sphere, a spherical cavity, a liquid-filled sphere, and an elastic sphere.

The significance of scattered waves in seismology is that it can be used to detect the attributes of the host medium and/or the properties of the scatterers. It is widely believed that coda waves, which are a train of waves following the arrival of the direct wave, are generated by the scattering from numerous scatterers in the earth medium. In the past twenty years, hundreds of studies have been carried out trying to use coda waves to obtain information about the earth medium. For example, coda waves have been intensively used to estimate the quality factor of the earth medium (Aki and chouet 1975; Jin and Aki, 1986). Besides, people also used coda waves to constrain the properties of the scatterers, such as the scattering turbidity or mean free path (Dainty et al, 1987; Sato, 1978), the scatterer position (Ogilvie, 1988; Nishigami, 1991), and the scatterer size (Liu et al., 1994))

In this study, the scattering characteristics of a small shallow subsurface sphere was investigated by calculating the synthetic seismograms in different positions on the surface. The purpose of this study is to find out if the scattered waves recorded by an array of receivers can be used to locate the scatterer. The scattering responses used in this study are obtained from Mie theory (Tie, 1987)

2. The method

2.1 General description

The method used in this study follows the modeling technique described by Ogilvie (1988) and Craig et al (1991). Here I give a brief summary of this method. After the occurrence of an earthquake, the wavelet radiated from the earthquake will finally arrive at the recording system. This wavelet is called the direct wave. In addition to this direct wave, the wavelets scattered by numerous scatterers will also be received by the recorder. During the traveling from the source to the receiver, the direct wavelet (U_{sou}) is modified by the impulse response of anelastic attenuation (ATN_{ab}), scattering attenuation (ATN_{sc}), the scalar amplification factor (GEO), instrument response (INS) and free surface effect (SUR). For the scattered wavelets, there is an additional modification factor, i.e., scattering response from scatterers (SCA). In a simple formula, the total displacement fieldin the recorder is

$$U_{rec} = [U_{sou} * ATN_{ab} * ATN_{sc} * INS] \bullet GEO \bullet SUR + \sum_{i=1}^{N} [U_{sou(i)} * ATN_{ab(i)} * ATN_{sc(i)} * SCA_i * INS] \bullet GEO_i \bullet SUR_i \qquad (1)$$

where * represents convolution, and • represent the product. The first term on the right-hand side of Equation (1) is the direct wavelet, and the second term is the superposition of scattered wavelets from all scatterers.

In our modeling, rather than using convolution in the time domain, all the operations are performed in the frequency domain so that convolution is a simple product. For each possible ray, we first calculate the overall spectral response by multiplying individual spectra, and then apply inverse Fourier transform to this overall spectral response to get the corresponding wavelet. The wavelet can be positioned on the in the synthetic seismogram based on the total time it needed to travel from the source to the receiver.

2.2 Computation of individual response spectrum

Source spectrum In this study we assume an explosive source. The source displacement spectrum was obtained from the explosive source model of Blake(1952). His study suggests that for a

spherical cavity subjected to a pressure step function, the far field wavelet is given by

$$U_{sou} = \frac{C_1 P_0 a^2}{r} \exp(-C_2 \tau) \sin(\omega_0 \tau) \qquad (2)$$

where C_1 and C_2 are constants that are functions of the density and Poisson's ratio of the medium, r is the distance from observation point to the cavity center, P_0 is the pressure amplitude, a is the radius of the cavity, ω_0 is the resonant frequency of the cavity, and τ=t-r/c, t represents time and c is the wave velocity. To get the source spectrum from this wavelet, Fourier transform was used.

Anelastic and scattering attenuation The anelastic attenuation refers to the decay of amplitude due to intrinsic absorption. The response spectra of anelastic attenuation is dependent on the intrinsic quality factor, Q_i, and may be written as:

$$S_{ab} = S_0(f) \exp(-\frac{\pi f}{Q_i} T) \qquad (3)$$

where T is the total travel time from source to receiver, f is frequency, and $S_0(f)$ defines the spectral amplitude at the source. The quality factor Q_i is generally assumed to be a constant. The phase response is obtained by assuming a causal wavelet.

Scattering attenuation is used to quantify the amplitude decay caused by the energy transformation from incident wave to scattered waves. We didn't consider this effect in our study because only one scatterer is present in the model.

Free-surface effect, geometrical spreading and instrument response When a wave strikes on a free surface, the displacement amplitude observed on the surface is different from the confined amplitude of the incident wave. This free-surface effect is corrected based on the equations provided by Ben-Menahem and Singh (1981).

For the incident and reflected plane waves, the geometrical spreading effect may be ignored. However, for the waves scattered from the small sphere, the displacement amplitude is decreased by spherical divergence. Assuming the radius of the scatterer is a_{sca}, and the distance from the

scatterer to the receiver is r, then during the travel from the scatterer surface to the receiver the displacement amplitude attenuated by the geometrical spreading is in a factor of a_{sca}/r.
Instrument response is certainly an important factor to affect the characteristics of the synthetic coda. However, in order to make our modeling to be comparable to the seismograms recorded from different types of instrument, instrument response is not included in our simulation. If it is required later, convolution of this result with a specific instrument response can be used to find the instrument-modified synthetic seismogram.

Scattering response Tie (1987) conducted a through study on the scattering of P wave by a spherical obstacle. Wu and Aki (1985) studied the scattering characteristics of a sphere using equivalent source method. The scattered wavelets have been used to model the generation of coda waves (Craig et al. 1991; Tie and Long, 1992). We also studied the case of S-wave scattering by an spherical obstacle using Mie theory. The main findings from these studies are (1) the amplitude of scattered wavelet varies strongly with the scattering angles. This variation is dependent on both the ka value and the heterogeneity parameters (2) For large ka (>1) and velocity type scattering (Wu and Aki, 1985), the largest amplitude of scattered wavelet occurs in the forward direction, and the smallest amplitude occurs in the backward direction. (3) For small ka and impedance type scattering, the largest amplitude occurs in the backward directions, and there is little scatting in the forward direction. (4) The shape of scattered wavelet also varies with scattering angle. In the forward direction, only one simple wavelet was observed (Figure 2 of Tie and Long, 1992). In the backward direction, multiple arrivals were found, which are caused by the multiple surface reflections of shear and/or P-wave inside the sphere.
In this study, the scattering response was obtained based on Mie's theory. Figure 1 shows the scattering amplitude variation with the scattering angle for the case when the incident wave is a plane P wave. Figure 2 is the case that the incident wave is a plane S wave. In these figures, the heterogeneity contrasts in P velocity, S velocity, and density are –0.3, -0.5, -0.5 respectively, which forms an impedance-type scattering object. We see that for intermediate and small ka (<2) the most significant scattering occurred in the backward direction. The largest amplitude of scattered wave increases with the increase of ka value. For ka equal to 0.1, the largest amplitude

of scattered wave is about 0.3~0.7 percent of the incident wave; while for ka equal to 1 and 5, the largest amplitude of the scattered wave becomes about 10~25 percent and 15~60 percent of the incident wave, respectively.

3. The Model

In our model, a teleseismic P wave was used as the incident wave. The frequency content and amplitude of the incident wave are obtained by assuming the explosion source has a spherical cavity radius of 6 meter and pressure amplitude of 1.5e05 Pa. The receivers are distributed as an 8 by 8 array on the surface. The scatterer is a small spherical obstacle with a radius of 5 meters. The position of the scatterer relative to the receivers varies in order to see how this change affects the scattered field. Figure 1 shows one case where the scatterer is centered below the receiver array.

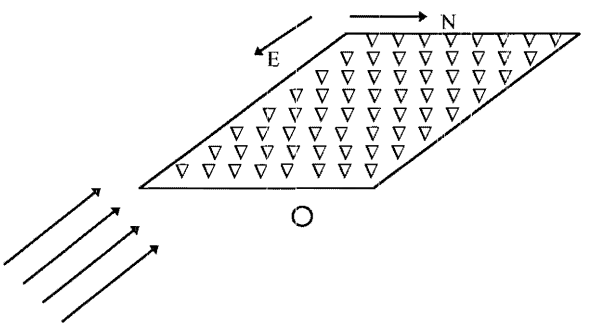

Figure 3. A plane P wave strikes on the record array

When the incident P wave passes through the small scatterer, scattered wavelets (both P and S wave) are generated. Besides, when the incident P wave strikes on the free surface, secondary plane P and SV waves are also generated due to reflection. These reflected waves will go back to the scatterer and resulted in another set of scattered waves. Therefore, three types of waves are recorded by the receivers. One type is the direct wave, the second type is the scattered waves due to the incident P wave, and the third type is the scattered waves due to the reflected waves.
The parameters used in this study are as follows:

- The incident wave comes from the southeast direction (azimuth=-45°) with a incident angle of 45°.

- The recorder array is distributed in a 22 by 22 m^2 area, the interval between the geophones is about 3 meters.
- The scatterer is a spherical inhomogeneity with the contrast in P velocity, S velocity, and density of –0.3, -0.5, -0.5 respectively.
- The host medium is uniform which has a P velocity of 1500m/s, an S velocity of 870m/s, and an density of 2670 kg/m^3. The intrinsic quality factor for the host medium is 1000.

4. The synthetic seismogram

Synthetic seismograms are generated for the scatterer in two different positions. One position is that the scatterer is centered below the array of receivers, and another position is that the scatterer is off away from the recording geophones. Figure 4 shows synthetic seismogram for the former case. In this figure, the three components, i.e. vertical, north-south, and east-west components, are shown in separate diagrams and the direct wave is truncated to show the scattered wave more clearly. The scattering from the small scatterer displays the following characteristics:

- The amplitude of scattered wave is much smaller than the direct wave. The amplitude ratio between scattered wave and direct wave is about 1/15.
- The horizontal components have larger amplitude than the vertical component. This phenomenon is caused by the fact that the scattered wave impinges on the free surface at very small incident angle (the angle between the incident direction and vertical). Because the scattered P wave is very close to the direct wave in time, the main compositions of the coda wave are shear waves. For the shear wave incidence and small incident angle, the free surface effect makes the amplitude of horizontal components larger than the vertical component.
- The forward scattering has relatively smaller amplitude than the backward and sideways scattering. This feature could attribute to that the scatterer has impedance-type heterogeneity parameters.

Synthetic seismograms were also calculated for the case where the scatterer is off away from the recording array. In this case, the scatterer is placed in the southeast of the recording system and the horizontal distance between the scatterer and the center of the array is 56 meters. The

calculated 3-component seismograms are shown in Figure 5. Comparing this figure with Figure 4, we found that this figure display some different features:

- The amplitude of scattered wave is smaller than the case where the scatterer is centered below the receivers. The amplitude ratio between them is about 1/5. This change is partially caused by the difference in the geometrical spreading factor and partially caused by the difference in scattering angle, because all the geophones in this case are in the forward direction
- As expected, a quite similar pattern was observed for the traces recorded by all the geophones.
- Contrary to Figure 4, the vertical component in this figure has larger amplitude than the horizontal components. This difference is resulted from the change in the incident angle of the scattered wave, because in this case the scattered wave has much larger incident angle than that of Figure 4.

To test if the scattered waves recorded by an array of receivers can be used to locate the scatterer, we need to find out if those scattered waves can still be identified if the background noise is also present in the seismogram. For this purpose, we insert a background noise into the simulated seismogram by the convolution between them. Figure 6 shows the background noise we used, and Figure 7 is one result of the convolution. Figure 7 is obtained through the convolution between the background noise and the third column of the vertical trace in Figure 5. It is found that the traces in Figure 7 are quite similar to the noise trace, which is a result of the large impulse of the incident wave. Due to the small amplitude of scattered waves, it may be very difficult to use the scattered waves to locate the scatterer.

5. Summary

In this study, the scattering characteristics of a small spherical inhomogeneity were investigated. Synthetic seismogram was calculated based on its scattering response. It is found that the scattered wave has much smaller amplitude than that of incident wave, and therefore the locating of a small scatterer based on the scattered wave may not give satisfactory result.

References

Aki, K. and Chouet, B., Origin of coda waves: source, attenuation and scattering effects. *J. Geophys. Res.*, 80, 3322-3342, 1975.

Blake, F.G. Spherical wave propagation in solid media. *J Acoust. Soc. Am.*, 24, 211-215, 1952.

Ben-Menahem, A. and Sign, S.J. Seismic wave and source. Springer-Verlag, New York, 1981.

Craig M.S., Long, L.T., and Tie, A. Modeling the seismic P coda as the response of discrete-scatterer medium. Phys. Earth Planet. Interiors, 67, 20-35, 1991.

Dainty, A. M., R. M. Duckworth, and A. Tie, Attenuation and backscattering from local coda, *Bull. Seism. Soc. Am.*, 77, 1728-1747, 1987.

Jin, A. and Aki, K., Temporal change in coda Q before the Tangshan earthquake of 1976 and Haicheng earthquake of 1975, *J. Geophys. Res.*, 91, 665-673, 1986.

Liu, E., S. Crampin, and J. Hudson. Diffration of seismic waves by cracks with application to hydraulic fracturing. *Geophysics*, 62, 253-265, 1994.

Nishigami, K., A new inversion method of coda waveforms to determine spatial distribution of coda scatterers in the crust and uppermost mantle, *Geophys. Res. Lett.* 18, 2225-2228, 1991.

Ogilvie, J. S., Modeling of seismic coda, with application to attenuation and scattering in southeastern Tennessee, M.S. Thesis, Georgia Institute of Technology, Atlanta, Georgia, 1988.

Sato, H., Mean free path of S-wave under the Kanto district of Japan, *J. Phys. Earth*, 26, 185-198, 1978.

Tie, A., 1987, On scattering of seismic waves by a spherical obstacle, Phd Dissertation at School of Geophysical Sciences, Georgia Tech., 1987.

Tie, A. and Long, L.T. The character of a scattered wavelet: a spherical obstacle embedded in an elastic medium. *Seismological Research Letters*, 63, No 4, 515-523, 1992.

Wu, R. S. and Aki, K., Scattering characteristics of elastic waves by an elastic heterogeneity, *Geophysics*, 50, 582-595, 1985.

Ying C.F. and Truell R. Scattering of plane longitudinal wave by a spherical obstacle in an isotropically elastic solid. *J Appl. Phys.*, 27, 1086-1097, 1956.